Mechanical Systems and Signal Processing 204 (2023) 110762

Contents lists available at ScienceDirect

Mechanical Systems and Signal Processing

journal homepage: www.elsevier.com/locate/ymssp

Simulation of non-stationary and non-Gaussian stochastic processes by the AFD-Type Sparse Representations

Ying Zhang [a], Wei Qu [b], He Zhang [c], Tao Qian [d,*]

[a] Department of Engineering Science, Faculty of Innovation Engineering, Macau University of Science and Technology, Macau 999078, China
[b] College of Sciences, China Jiliang University, Hangzhou 310018, China
[c] Beijing International Center for Mathematical Research, Peking University, Beijing 100871, China
[d] Macau Center for Mathematical Sciences, Macau University of Science and Technology, 999078, Macao Special Administrative Region of China

ARTICLE INFO

Communicated by I. Kougioumtzoglou

Keywords:
Adaptive fourier decomposition
Non-Gaussian stochastic process
Non-stationary
Karhunen–Loève expansion
Polynomial chaos

ABSTRACT

Simulation of a stochastic process to simultaneously meet a given marginal distribution condition and be compatible with a given covariance function is a well-known problem called the two-match problem in the sequel. We propose the adaptive Fourier decomposition (AFD) type methods as constructive steps to solve the two-match problem. AFD-Type methods used in the physical domain (e.g., time or frequency) are replacements of the Karhunen–Loève expansion, or spectral decomposition, in general, while, when being used in the probability space are replacements of the polynomial chaos or other types of chaos methods. The AFD-Type methods in both circumstances play the role of an approximation. Being compared with the Karhunen–Loève expansion, the proposed AFD-Type methods do not need to compute out the eigenvalues and eigenfunctions of the kernel integral operator defined by the target covariance function, while compared with the polynomial chaos or other chaos methods the AFD-Type methods offer a great deal of flexibility and efficiency. The proposed methods can be applied to stationary and non-stationary, weakly, and strongly non-Gaussian stochastic processes. We provide several examples to show effectiveness and efficiency of the AFD-Type methods.

1. Introduction

Stochastic processes are often used as mathematical models of systems in various fields, such as finance [1,2], biochemical engineering [3], and stochastic mechanics [4]. Generally, owing to the central limit theorem and simplicity of the form, most stochastic processes are studied based on the Gaussian distribution. There exist several methods to simulate Gaussian stochastic processes. For example, spectral representation, initially developed for stationary Gaussian stochastic processes [5], is implemented in the frequency domain. The Karhunen–Loève (KL) expansion is usually used in the simulation of stationary and non-stationary Gaussian stochastic processes [6]. Usually, the KL method requires the time or spatial domain to be within a compact set. In the stationary Gaussian stochastic process case, the KL expansion is reduced to the spectral representation.

However, the observed data may exhibit prominent non-Gaussian characteristics. Non-Gaussian models are encountered in many fields of applied science and engineering, such as astronomy [7], economy [8], environment [9–11], mechanics [12], and hydrology [13]. There have been two classes of simulation schemes for generating sample functions of non-Gaussian stationary

* Corresponding author.
E-mail addresses: cnuzhangying@163.com (Y. Zhang), quwei2math@qq.com (W. Qu), zhanghe@bicmr.pku.edu.cn (H. Zhang), tqian@must.edu.mo (T. Qian).

https://doi.org/10.1016/j.ymssp.2023.110762
Received 2 May 2023; Received in revised form 27 July 2023; Accepted 6 September 2023
Available online 16 September 2023

random processes. The first class generates realizations of stochastic processes based on their prescribed lower-order moments (e.g., mean, variance, skewness, and kurtosis) and power spectral density function (PSDF). This class is suitable for the simulation of wind and wave loads, and significant work has been done in this area [14,15]. The second class generates realizations of stochastic processes based on their prescribed marginal probability distribution and power spectral density function. The primary method in this class is the spectral representation method (SRM) [16], which relies on translation process theory [17]. This method iteratively updates the PSDF of the underlying Gaussian process until the PSDF of the non-Gaussian sample function converges to the desired target. However, this algorithm causes the underlying "Gaussian" process to deviate from Gaussianity as the iterations progress, leading to "incompatibility" between the target PSDF and the target marginal distribution of the non-Gaussian stochastic process [18]. Later, this issue was addressed in the article [19], particularly for strongly non-Gaussian distribution. The proposed simulation technique in [20] improves the underlying Gaussian PSDF iteratively by relying on the computed non-Gaussian PSDF at each iteration, thus eliminating the need to generate sample functions. The difficulty of the second class in simulating non-Gaussian random processes is that all joint distribution functions are required to characterize the non-Gaussian properties fully. SRM models, however, will not be considered in this work. Besides, other techniques have also been developed for the simulation of stationary and non-stationary non-Gaussian stochastic processes, such as KL iterative algorithms are proposed in [21,22] to update the non-Gaussian expanded random process, and they can be applied to highly skewed non-Gaussian marginal distribution functions. Besides, the Polynomial Chaos (PC) method commonly represents stationary and non-stationary non-Gaussian random processes. A procedure is presented in [23] for developing a representation of lognormal stochastic processes via the polynomial chaos expansion. Such as this paper [24] proposes a general method to generate simulated paths of non-Gaussian homogeneous random on a Hermite polynomial expansion, given the spectral measure of the random process and either the marginal distribution or statistical moments. In paper [25], the non-Gaussian process is represented as a polynomial transformation of an appropriate Gaussian process. The target correlation structure is decomposed according to the KL expansion of the underlying Gaussian process. Zheng et al. propose a method [26] to generate random samples matching the covariance and non-Gaussian marginal distribution functions. The basic idea is to generate random samples satisfying the target marginal distribution and then develop an iterative algorithm to reach the target covariance function. The accuracy and efficiency of the simulation only depend on matching the target covariance function. However, applying random samples to practical problems is usually not convenient. Zheng et al. use KL, PC, and KL+PC methods to expand the samples they obtain in the discrete form to the continuous form, enhancing the applicability of their results in [26].

The primary purpose of this work is to simulate a stochastic process that simultaneously satisfies a marginal distribution condition and a covariance condition, provided the two given conditions are compatible. We will not discuss in detail the well-posedness of such a problem in the present paper but assume that processes satisfying simultaneously the two given conditions exist. This paper will refer to such a problem as a "two-match" problem.

In this paper, we show a uniform methodology using the AFD-type methods to deduce continuous forms of random functions based on discrete samples, such as what is done by using KL and PC methods in, for instance, [26]. The AFD-type algorithms originated from signal decomposition into basic signals of meaningful positive instantaneous frequencies formulated in the complex Hardy spaces [27]. The formulation is based on generalized backward shift operators. As an approximation method, it was later extended to general Hilbert spaces with a dictionary, the latter being called pre-orthogonal adaptive Fourier decomposition, or POAFD in brief [28,29].

There exist three main matching pursuit algorithms. According to the order of increased efficiency, they are listed as the (pure) greedy algorithm, orthogonal greedy algorithm [30], and POAFD. In the classical Hardy spaces, POAFD is identical to AFD (or, more specifically, Core AFD). Lately, stochastic counterparts of the deterministic AFD methods were developed [31]. This paper mainly uses stochastic pre-orthogonal adaptive Fourier decomposition (SPOAFD) and POAFD-Chaos. The purpose or main contribution of the present paper is to solve the two-match problem using the AFD-Type methods, which demonstrate great power and flexibility over the pre-existing methods [21,25]. For the first time, they are introduced to and implemented in the related problems. The AFD-related methods used to solve the two-match problem in this paper are three-fold based on Zheng's sampling. The first fold is to use Stochastic Core AFD (taking the real part afterward) or SPOAFD based on the Poisson kernel dictionary to replace the KL expansion as used in [26]. Since the SPOAFD methods do not need to compute the eigen-pairs, they significantly save the relevant computation cost and obtain the same convergence rate $O(n^{-1/2})$. The literature [32] establishes SAFD-type methods but does not give application examples, nor numerical experiments. The second fold further expands the random coefficients c_ks in the representation formula (24) produced in the first fold. This task is usually done by using polynomial chaos [24]. What we do, instead, is to use rational chaos, or more generally AFD-Chaos, to replace PCs. At this point, we introduce our new AFD-Type method named AFD-Chaos, that including Rational Chaos (RCs). The characteristic property of the new chaos methods is an adaptive selection of dictionary parameters to maximize the modules of expectations of products of two random variables. In the twin paper [33], the theory of AFD-Chaos, including Rational Chaos (RCs), is systematically developed. The third-fold contribution of the paper is direct expansion using an adaptive system in the probability space defined similarly with one to the time or the spacial space (SAFD types). This strategy is under the idea that a random field may also be expanded using a basis in the probability space (as using PCs in [25]). For a Hilbert space, there may exist more than one dictionary. One can, therefore, select a dictionary for a specific task. For instance, one uses the Szegö kernel dictionary for instantaneous frequency decomposition of signals and obtains an adaptive Takenaka-Malmquist system [27]. To solve a Dirichlet boundary value problem, one uses the Poisson kernel dictionary, and to solve an initial value problem with the heat equation, one uses the heat kernel dictionary. Once one obtains an efficient decomposition of the boundary value or the initial value by the "lifting up" method, using the potential solution formulae and the semi-group property of the kernels, one immediately obtains the solution to the corresponding problem [34]. A suitably selected dictionary gives rise to an efficient solution. AFD-Chaos methods, too, enjoy flexibility and efficiency through adaptive selection of dictionary

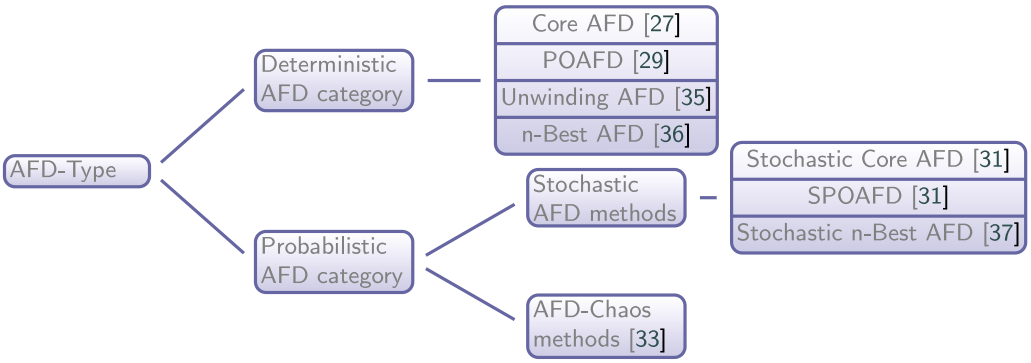

Fig. 1. Specific classification of AFD-Type sparse representations (see [35–37]).

and dictionary elements according to the task taken. The specific AFD-Type classification can refer to Fig. 1. We provide several examples showing that SPOAFD and POAFD-Chaos are competitive with the traditional KL and PC methods.

The writing plan of the paper is as follows. The KL and Hermite PC expansion are briefly reviewed in Section 2 for the self-containing purpose. In Section 3, the SPOAFD and POAFD-Chaos methods are sketched. In Section 4, SPOAFD and POAFD-Chaos are used in simulating the non-Gaussian stochastic processes based on Zheng's discrete samples. In Section 5, we include four examples to show the feasibility and high accuracy of the proposed algorithms. In Section 6, we give conclusions.

2. Existing expansion of stochastic process

This section reviews some main existing expansion methods of a stochastic process. Given a probability space $(\Omega, \mathcal{F}, P)$, we focus on a second-order stochastic process $\{f(t,\omega),(t,\omega)\in\mathcal{T}\times\Omega\}$ that belongs to the Bochner space defined below, where $\mathcal{T}$ corresponds to the time domain or the spatial field in general.

Definition 1. The Bochner space $L^2(\mathcal{T},\Omega)$ [31,38] is defined to be the Hilbert space consisting of all $L^2(\mathcal{T})$-valued random variables $f:\mathcal{T}\times\Omega\to\mathbb{R}$ satisfying

$$\|f\|^2_{L^2(\mathcal{T},\Omega)} := \int_\Omega\int_{\mathcal{T}} |f(t,\omega)|^2\, dt d\mathbb{P}(\omega) < \infty. \tag{1}$$

For brevity, we also write $\mathcal{N} = L^2(\mathcal{T},\Omega)$. The Bochner space $\mathcal{N}$ is a Hilbert space with the inner product defined through Bochner integral [39,40]. For processes in $\mathcal{N}$, we introduce the covariance function $\mathbf{C}(s,t) := \mathbb{E}_\omega[f(s,\cdot)f(t,\cdot)]$. In this paper, we focus on the problem of generating stochastic processes satisfying the given marginal distributions and covariance function. The KL expansion approaches the problem by expanding the stochastic process into an infinite sum of variable separation functions. Roughly speaking, if one of the two spaces, namely $\mathcal{T}$ or Ω, has a "basis", then one can, through working out the necessary details, eventually have an expansion of the form

$$f(t,\omega) = \mu(t) + \sum_{k=0}^{\infty} \xi_k(\omega) g_k(t), \tag{2}$$

where $\{\xi_k(\omega)\}_{k=0}^\infty$ is a set of random variables and $\{g_k(t)\}_{k=0}^\infty$ is a set of deterministic functions, $\mu(t)$ is the mean of stochastic process $f(t,\omega)$, i.e. $\mu(t)=\mathbb{E}_\omega[f(t,\cdot)]$. One often works on the corresponding stochastic processes with zero mean, that is, $f_0(t,\omega) := f(t,\omega)-\mu(t)$. In later discussion, for simplicity, $f(t,\omega)$ and $f_0(t,\omega)$ are alternatively written as $f(t)$ and $f_0(t)$, respectively, hiding the sample path ω.

2.1. Karhunen–Loève expansion

The KL expansion is one of the most commonly used methods to represent stochastic processes. Consider the integral operator $\mathcal{I}$ using the covariance $\mathbf{C}(s,t)$,

$$\mathcal{I}(\varphi)(s) := \int_{\mathcal{T}} \mathbf{C}(s,t)\varphi(t)dt,\ \ s,t\in\mathcal{T},\ \ \varphi(t)\in L^2(\mathcal{T}). \tag{3}$$

The solutions of the homogeneous Fredholm integral equation of the second kind

$$\int_{\mathcal{T}} \mathbf{C}(s,t)\varphi_k(t)dt = \lambda_k\varphi_k(s),\ \ s\in\mathcal{T}, \tag{4}$$

give rise to eigenvalues and eigenfunctions of the integral operator I. If the covariance function $\mathbf{C}(s,t)$ meets the conditions required by the Mercer Theorem [41] then it has the following decomposition:

$$\mathbf{C}(s,t) = \sum_{k=1}^{\infty} \lambda_k \varphi_k(s)\varphi_k(t), \ \ s,t \in \mathcal{T}, \tag{5}$$

where φ_k's are the orthonormal eigenfunctions in $L^2(\mathcal{T})$, and the positive λ_k's are in the descent order. Taking $g_k(t) = \sqrt{\lambda_k}\varphi_k(t)$ in (2), we obtain the KL expansion in $\mathcal{N}$

$$f_0(t,\omega) = \sum_{k=1}^{\infty} \sqrt{\lambda_k}\varphi_k(t)\xi_k(\omega), \tag{6}$$

where $\{\xi_k(\omega)\}_k$ are the random variables given by

$$\xi_k(\omega) = \frac{1}{\sqrt{\lambda_k}} \int_{\mathcal{T}} f_0(t,\omega)\varphi_k(t)dt, \tag{7}$$

which satisfy $\mathbb{E}_\omega[\xi_k] = 0, \ \ \mathbb{E}_\omega[\xi_k\xi_m] = \delta_{km}$, where δ_{mn} is the Kronecker-delta function. If the process is Gaussian, then $\xi_j \sim N(0,1)$ i. i. d. In practical applications, one adopts a finite truncated series expansion

$$\hat{f}_0(t,\omega) = \sum_{k=1}^{n} \sqrt{\lambda_k}\varphi_k(t)\xi_k(\omega). \tag{8}$$

Notice that the analytical solution of the integral Eq. (4) is not generally available, and one needs to solve the eigenvalue problem numerically. Besides, the set of basis functions $\{\sqrt{\lambda_k}\varphi_k(t)\}$ are chosen as the leading eigenfunctions, which depend only on the covariance function. In other words, we trade off the sparseness of the representation for the uniformity of the expansion formula (8). Thus, avoiding solving eigenvalue problems and looking for sparse representations are two primary motivations for considering AFD-Type methods. Since the polynomial chaos expansion inspires the idea of the AFD-Chaos, we will briefly review the theory in the following subsection.

2.2. Generalized polynomial chaos expansion

The terminology *generalized polynomial chaos* (gPC) was first introduced by Xiu et al. in [42], including Hermite polynomial chaos, Legendre polynomial chaos, and Jacobi polynomial chaos, etc. Referred to Xiu's book [43], we first review the concepts of strong and weak convergence of gPC. The strong and weak convergences are also known as the mean-square convergence and convergence in distribution, respectively.

Let Z be a random variable with cumulative distribution function (CDF) $F_Z(z) = P\{Z \le z\}$. For an integrable function g, there holds $\mathbb{E}_Z[g(Z)] = \int_{I_Z} g(z)dF_Z(z)$, where I_Z is the support of the random variable Z. Let

$$L^2_{dF_Z} = \left\{ g : I_Z \to \mathbb{R} \middle| \ \mathbb{E}_Z\left[g^2\right] < \infty \right\} \tag{9}$$

be the space of all mean-square integrable functions with norm $\|g\|_{L^2_{dF_Z}} = \left(\mathbb{E}_Z\left[g^2\right]\right)^{1/2}$. Let $\left\{\Psi_k(Z)\right\}_k$ be an orthogonal polynomial system of Z, that is,

$$\mathbb{E}_Z\left[\Psi_m(Z)\Psi_n(Z)\right] = \mathbb{E}_Z\left[\Psi_n^2(Z)\right]\delta_{mn}. \tag{10}$$

The strong convergence is formulated as follows.

Proposition 1 (*[43]*). *Let $\{\Psi_k(Z)\}_k$ be a basis of $L^2_{dF_Z}$ and $g(Z) \in L^2_{dF_Z}$ a mean-square integrable function. Set*

$$g_N(Z) = \sum_{k=0}^{N} \hat{g}_k\Psi_k(Z) \in \mathbb{P}_N(Z), \quad \textit{where } \hat{g}_k = \mathbb{E}_Z\left[g(Z)\Psi_k(Z)\right]/\mathbb{E}_Z\left[\Psi_k^2(Z)\right], \tag{11}$$

and $\mathbb{P}_N(Z)$ denotes the space of polynomials of Z of degree up to $N \ge 0$. Then we have $\|g(Z) - g_N(Z)\|_{L^2_{dF_Z}} \to 0$ as $N \to \infty$.

In practice, however, g may not be in $L^2_{dF_Z}$, and the strong convergence does not hold. In such a case, the gPC expansion may converge in a weak sense. Recall that, for any random variable Y and Z, there hold $U = F_Y(Y) = F_Z(Z)$, where $U \sim \mathcal{U}(0,1)$. Thus, we have the representation $Y = F_Y^{-1}(U) = F_Y^{-1}\left(F_Z(Z)\right)$, where

$$F_Y^{-1}(u) := \inf\{y : F_Y(y) \ge u\}, \ 0 < u < 1.$$

(see, for instance, Proposition 2.11 of [43]). For sample-based gPC, that is, the explicit CDF F_Y being unavailable, we can replace F_Y by the corresponding empirical CDF, which is a step function.

Proposition 2 (*Theorem 5.7 of [43]*). *Let Y be an arbitrary random variable of a finite second moment and CDF $F_Y(y)$. Let Z be a random variable with CDF $F_Z(z)$. Set*

$$Y_N = \sum_{k=0}^{N} a_k\Psi_k(Z), \quad \textit{where } a_k = \frac{\mathbb{E}\left[Y\Psi_k(Z)\right]}{\mathbb{E}_Z\left[\Psi_k^2\right]} = \frac{\mathbb{E}_Z\left[F_Y^{-1}(F_Z(Z))\Psi_k(Z)\right]}{\mathbb{E}_Z\left[\Psi_k^2\right]}. \tag{12}$$

Then Y_N converges to Y in probability. The convergence is also in distribution.

As an example of gPC, the homogeneous chaos, also called the Hermite polynomial chaos, was first proposed by Wiener [44], which uses the Hermite polynomials as the orthogonal system of Gaussian random variables. Let $H_j(Z)$ be the j-order Hermite polynomial satisfying

$$H_j(Z) = (-1)^j \frac{\rho^{(j)}(Z)}{\rho(Z)}, \tag{13}$$

where $\rho^{(j)}(t)$ is the jth derivative of the Gaussian density $\rho(t) = \frac{1}{\sqrt{2\pi}} e^{-\frac{t^2}{2}}$.

Let $f_0(t,\omega)$ be the corresponding zero-mean stochastic process. For each fixed t, $f_0(t)$ is a random variable. Introducing the corresponding CDF $F^{-1}_{f_0(t)}(u)$, we again use the relation

$$f_0(t) = F^{-1}_{f_0(t)}(U) = F^{-1}_{f_0(t)}\left(F_Z(Z)\right), \tag{14}$$

and the stochastic process $f_0(t)$ then possesses a Herimite PC expansion in the probability sense

$$f_0(t) = \sum_{k=0} a_k(t) H_k(Z) = a_0(t) + a_1(t)Z + a_2(t)(Z^2-1) + a_3(t)(Z^3-3Z) + \cdots, \tag{15}$$

where

$$a_k(t) = \frac{\mathbb{E}\left[f_0(t)H_k(Z)\right]}{\mathbb{E}_Z\left[H_k^2(Z)\right]} = \frac{E_Z\left[F^{-1}_{f_0(t)}(F_Z(Z))H_k(Z)\right]}{\mathbb{E}_Z\left[H_k^2(Z)\right]},\ t \in \mathcal{T}. \tag{16}$$

Achieving weak convergence of a stochastic process expanded by PC requires determining its PC coefficients $a_k(t)$ (16) at each time step. The numerical implementation involves fixing the variable t, discretizing the stochastic process into a set of random variables, and calculating the corresponding inverse CDF. For gPC, unlike KL expansions, the basis functions are orthogonal polynomials of random variable Z over Ω, and we do not need to solve the eigenvalue problems. Adopting the idea of gPC, Section 3.2 presents our innovative approach to simulating stochastic processes with sparse representations.

3. AFD-Type sparse representations

In recent literature, there appear a variety of sparse representations referred to as adaptive Fourier decomposition (AFD) type methods that do not fall into the greedy algorithm of common sense. Although they also use energy-matching pursuit, they adopt different iterative designs. Compared with greedy algorithms, AFD methods directly obtain orthogonal sparse representations with greedier effects in the one-by-one parameter selection pattern than that of the greedy algorithm. As a particular feature, they address attainability at each step of the global optimal parameter selection and give rise to positive frequency decomposition as Fourier expansions do [27,28].

The AFD-type representations are divided into deterministic and probabilistic categories as briefly classified in Fig. 1. They are also overall called AFD-type methods, inducing the AFD-Chaos through the transform methods used in (12) and (16). Below we provide detailed information for the AFD-Type methods used in this paper.

3.1. Expansion by SPOAFD

We now introduce the SPOAFD method aiming at solving the two-match problem with KL expansion as the baseline. Sparse representation of Hilbert space is often under the assumption that the space has a *dictionary* that, by definition, is a collection of unimodular elements whose span is dense in the Hilbert space. By a *pre-dictionary*, we mean a collection of elements (not necessarily unimodular) whose span is dense in the Hilbert space. We adopt the parameter set $\mathbf{D}$, the open unit disc in the complex plane with $\partial\mathbf{D}$ being the boundary of $\mathbf{D}$.

We take $\mathcal{T} = \partial\mathbf{D}$ as the time domain, and consider the $L^2(\partial\mathbf{D})$-dictionary of the form $\{K_q\}_{q\in\mathbf{D}}$, i.e., parameterized by elements in D. (A typical example is the Poisson kernel (23)) We recall that the dictionary satisfies the *boundary vanishing condition* (BVC) [27] if any but fixed function $f \in L^2(\partial\mathbf{D})$ there holds

$$\lim_{q\to\partial\mathbf{D}} |\langle f, E_q\rangle_{L^2(\partial\mathbf{D})}| = 0, \tag{17}$$

where $\langle\cdot\rangle$ denotes the inner product, and E_q is normalized kernel

$$E_q = \frac{K_q}{\|K_q\|_{L^2(\partial\mathbf{D})}}, q \in \mathbf{D}.$$

It is necessary to introduce the notion of *multiple kernels* [31]. For an n-tuple $(q_1,\ldots,q_n)$ of elements in $\mathbf{D}$, we denote the multiple of q_k in the k-tuple $(q_1,\ldots,q_k)$ as $\ell(k)$, $1 \le k \le n$. Then, the corresponding kth multiple kernel is defined as

$$\tilde{K}_{q_k} = \left[\left(\frac{\partial}{\partial\overline{q}}\right)^{(\ell(k)-1)} K_q\right]_{q=q_k},\ k = 1,2,\ldots,n, \tag{18}$$

where $\frac{\partial}{\partial \overline{q}}$ is interpreted as a directional derivative and $\overline{q}$ is the complex conjugate of q. We also use E_{q_k} to denote the corresponding normalized kernel, that is,

$$E_{q_k} = \frac{\tilde{K}_{q_k}}{\|\tilde{K}_{q_k}\|_{L^2(\partial \mathbf{D})}}, \ k = 1, 2, \dots, n. \tag{19}$$

Multiple kernels are generated from performing the *stochastic* pre-orthogonal maximal selection principle (SPOMSP) [31]. With only a little difference, the notation E_k is preserved for a general entry in the orthonormal system $(E_1, \dots, E_n)$, and E_n^q means that the last used parameter in E_n is q. The generating process consists of an optimization step deciding a point $q \in \mathbf{D}$ and an orthogonalization step to ensure the orthogonality of the basis functions. We summarize the steps into the following proposition.

Proposition 3 (*[31]*). *Assume that the dictionary* $\{K_q\}$ *of* $L^2(\partial \mathbf{D})$ *satisfies BVC (17). Then for every* $f(t, \omega) \in \mathcal{N}$ *there exists* $q_k \in \mathbf{D}$ *such that*

$$q_k = \arg\sup_{q \in \mathbf{D}} \mathbb{E}_\omega \left| \langle f_0(\cdot, \omega), E_k^q \rangle \right|^2, \tag{20}$$

where the finiteness of the supreme is ensured by the Cauchy–Schwarz inequality, and $\{E_1, \dots, E_{n-1}, E_n^q\}$ *is the Gram–Schmidt (G-S) orthonormalization of* $\{E_1, \dots, E_{n-1}, \tilde{K}_q\}$.

The steps of G-S orthogonalization mentioned in Proposition 3 is computed through [29,45]

$$E_n = E_n^{q_n} = \frac{\tilde{K}_{q_n} - \sum_{l=1}^{n-1} \langle \tilde{K}_{q_n}, E_l \rangle E_l}{\sqrt{\|\tilde{K}_{q_n}\|^2 - \sum_{l=1}^{n-1} \left| \langle \tilde{K}_{q_n}, E_l \rangle \right|^2}}. \tag{21}$$

For each k, the quantity $\mathbb{E}_\omega |\langle f_0(\cdot, \omega), E_k^q \rangle|^2$ in (20) may be computed by [32]

$$\begin{aligned} \mathbb{E}_\omega \left| \langle f_0(\cdot, \omega), E_k^q \rangle \right|^2 &= \int_{\partial \mathbf{D}} \int_{\partial \mathbf{D}} \mathbb{E}_\omega \left[f_0(t, \omega) \overline{f_0(s, \omega)} \right] \overline{E_k^q}(t) E_k^q(s) dt ds \\ &= \int_{\partial \mathbf{D}} \int_{\partial \mathbf{D}} \mathbf{C}(s, t) \overline{E_k^q}(t) E_k^q(s) dt ds. \end{aligned} \tag{22}$$

Thus, the optimal parameters required for SPOAFD expansion are computed through the covariance function $\mathbf{C}(s, t)$. Although the resulting system $\{E_k\}$ by SPOAFD is not necessarily a basis, it generates efficient approximation to stochastic processes in $\mathcal{N} = L^2(\mathcal{T}, \partial \mathbf{D})$. Multiple choices of dictionary or pre-dictionary can be adopted according to the context and the purpose. In this paper, the pre-dictionary we adopt consists of the parameterized Poisson kernels $P_q(t)$,

$$P_q(t) = \frac{1 - |q|^2}{|q - e^{it}|^2}, \quad q \in \mathbf{D}, \quad t \in \partial \mathbf{D}, \tag{23}$$

and we develop the corresponding SPOAFD expansion for a stochastic process.

Theorem 1. *For any* $f(t, \omega) \in \mathcal{N}$, *its SPOAFD series is well-defined and converge to* $f(t, \omega)$ *in* $\mathcal{N}$. *That is, with the parameters* $\{q_k\}_k$ *selected under SPOMSP (20), possibly with multiplicity, there holds*

$$f_0(t, \omega) = \sum_{k=1}^{\infty} \langle f_0(\cdot, \omega), E_k \rangle E_k(t) = \sum_{k=1}^{\infty} c_k(\omega) \tilde{P}_{q_k}(t), t \in \partial \mathbf{D}, \tag{24}$$

where $\{E_k\}_{k=1}^{\infty}$ *is the G-S orthogonalization of the multiple kernels* $\{\tilde{P}_{q_k}\}_{k=1}^{\infty}$, *and* $\{c_k(\omega)\}_{k=1}^{\infty}$ *is the corresponding coefficient converted to the nonorthogonal basis* $\{\tilde{P}_{q_k}\}_{k=1}^{\infty}$.

In practice, we use a partial sum of the series in (24) to approximate $f_0(t, \omega)$:

$$\hat{f}_0(t, \omega) = \sum_{k=1}^{n} \langle f_0(\cdot, \omega), E_k \rangle E_k(t) = \sum_{k=1}^{n} c_k(\omega) \tilde{P}_{q_k}(t). \tag{25}$$

Under mild conditions on $f(t, \omega)$, the convergence rate of (25) is $O\left(n^{-\frac{1}{2}}\right)$ as proved in [31]. Notably, our method achieves the same convergence order as KL and provides a continuous analytical expansion for stochastic processes. The critical components of this approach involve performing G-S orthonormalization of the system and solving the coefficients of (24) via SPOMSP.

3.2. Expansion by AFD-Chaos

The gPCs inspire the creation of AFD-Chaos. To represent more general stochastic processes using AFD-Chaos, we are restricted here to concern weak convergence. For more details of AFD-Chaos, including the strong convergence case, we refer the reader to [33]. For later use, we denote $U(\omega)$ as the uniformly distributed random variable on $\partial \mathbf{D}$ with CDF $F_U(u) = P(U \le u) = u/2\pi$, $u \in \partial \mathbf{D}$.

Table 1
Different type expansions for stochastic processes.

Expanding system in different domains	Existing expansion methods of RP	Proposed new expansion methods of RP
Physical domain (e.g. time or space)	e.g. Mercer-KL $f_0(t,\omega)=\sum_k \sqrt{\lambda_k}\xi_k(\omega)\varphi_k(t)$	SPOAFD $f_0(t,\omega)=\sum_k \langle f_0(\cdot,\omega),E_k\rangle E_k(t)$
Probability space (chaos)	e.g. Hermite-PC $f_0(t,\omega)=\sum_k a_k(t)H_k(Z(\omega))$	POAFD-Chaos $f_0(t,\omega)=\sum_k g_k(t)E_k(U(\omega))$
mixture of physical and probability space	e.g. KL+PC $f_0(t,\omega)=\sum_k\sum_l a_{kl}\sqrt{\lambda_k}H_l(Z_k(\omega))\varphi_k(t)$	SPOAFD+AFD Chaos $f_0(t,\omega)=\sum_k\sum_l g_{kl}E_l(U(\omega))E_k(t)$

There are two choices to expand $f(t,\omega)$ by AFD-Chaos methods. The first is referred as *combination method* that is as the first step expanding it for in variable t by using a stochastic AFD methods [31], or any basis in the boundary L^2 space, including the one asserted by Mercer's Theorem (5) used in KL expansion (6), and get a series for each fixed sample path ω as a function of t :

$$f_0(t,\omega)=\sum_{k=1}^{\infty} c_k(\omega)E_k(t),$$

where $c_k(\omega)=\langle f_0(\cdot,\omega),E_k\rangle$. When SPOAFD is used, that is, we have $q_1,q_2,\ldots\in\mathbf{D}$ are selected according to the SPOMSP to produce the orthonormal system $\{E_k\}_{k=1}^{\infty}$. Then, as the second step, we further expand each $c_k(\omega)$ by using any AFD-Chaos methods adapted to the random variable $c_k(\omega)$. The parameters relevant to k are $q_n^{(k)}, n=1,2,\ldots$, selected according to

$$q_n^{(k)}=\arg\sup_q\left\{\mathbb{E}_\omega\left[\left|c_k(\omega)E_n^q(U(\omega))\right|^2\right]\;\middle|\; q\in\mathbf{D}\right\}. \tag{26}$$

where the computation of the inside expectation $\mathbb{E}_\omega\left|[c_k(\omega)E_n^q(U(\omega))]\right|^2$ is referred to (12), in which we replace Y by c_k, Z by U, Ψ_n by E_n^q, and $\mathbb{E}_Z\left[\Psi_n^2\right]$ simply by 1. In such a way, we get an expansion of $f(t,\omega)$ strongly converge in $\mathcal{N}$, while for each random coefficient c_k, we have an AFD-Chaos expansion with weak convergence. The literature [26] uses this two-step method, first expanding the random signal in t by KL and then expanding each of the coefficient random variables by Hermite PC. What we propose here is that both KL and PC may be replaced, respectively, by stochastic AFD methods and AFD-Chaos methods expansions.

The *POAFD-Chaos*, in contrast with the combination method, belongs to the AFD category and is formulated as follows. For any given $f(t,\omega)\in\mathcal{N}$, we have the optimal selections of the parameters

$$q_k=\arg\sup_q\left\{\sup_{t\in\partial\mathbf{D}}\mathbb{E}_\omega\left[\left|f_0(t,\omega)E_k^q(U(\omega))\right|^2\right]\;\middle|\; q\in\mathbf{D}\right\}, \tag{27}$$

where $\{E_1,\ldots,E_{k-1},E_k^q\}$ is the G-S orthonormalization of *stochastic Poisson kernel* $\{E_{q_1},\ldots,E_{q_{k-1}},P_{q_k}\}$, assuming that $q_1,\ldots,q_k$ are distinguished parameters. The orthonormalization formula is the same as (21). The randomized Poisson kernel is defined as

$$P_{q_k}(U(\omega))=\frac{1-|q_k|^2}{|q_k-e^{iU(\omega)}|^2},\quad q_k\in\mathbf{D},\quad U(\omega)\in\partial\mathbf{D}. \tag{28}$$

The validity of the SPOMSP (27) is based on the Time-Uniform Boundary Vanishing Condition [33]

$$\lim_{q\to\partial\mathbf{D}}\sup_{t\in\partial\mathbf{D}}\mathbb{E}_\omega\left[\left|f_0(t,\omega)E_k^q(U(\omega))\right|^2\right]=0.$$

The generated stochastic Poisson kernel orthonormal system $\{E_k\}$ satisfies

$$\mathbb{E}_\omega\left[E_k(U(\omega))\,E_l(U(\omega))\right]=\frac{1}{2\pi}\int_0^{2\pi}E_k(u)E_l(u)du=\delta_{kl}. \tag{29}$$

We can derive the following convergence theorem from the above conclusion and [33].

Theorem 2. *Let the stochastic process $f(t)\in\mathcal{N}$. Set $f_0(t)=f(t)-\mu(t),\mu(t)=\mathbb{E}[f(t)]$. Under a set of consecutively and maximally selected $\{q_k\}_{k=1}^{\infty}$ according to (27), we have a chaos expansion converging in probability*

$$f_0(t)=\sum_{k=1}^{\infty}g_k(t)E_k(U), \tag{30}$$

where the deterministic function $g_k(t)$ is determined by the orthogonality of the G-S orthonormalization of the selected stochastic Poisson kernels:

$$g_k(t)=\mathbb{E}_\omega\left[f_0(t)E_k(U)\right]. \tag{31}$$

In application, the random function $f(t)$ is approximated by truncated series

$$\hat{f}_0(t)=\sum_{k=1}^{n}g_k(t)E_k(U)=\sum_{k=1}^{n}h_k(t)P_{q_k}(U), \tag{32}$$

where $(h_1(t),\dots,h_n(t))$ and $(g_1(t),\dots,g_n(t))$ are converted to each other by the relevant transform matrices. Referred to [43] or [33], we note the computation formula of $g_k(t)$:

$$g_k(t)=\mathbb{E}_\omega\left\{\left[f_0(t)\,E_k(U)\right]\right\}=\frac{1}{2\pi}\int_0^{2\pi}\left[F^{-1}_{f_0(t)}\left(\frac{u}{2\pi}\right)\right]E_k(u)du. \tag{33}$$

Remark 1. Although we discuss the details based on stochastic Poisson kernel pre-dictionary over the unit circle, in the infinite time region, the stochastic Poisson kernels on the upper half plane and other kernel systems such as the stochastic heat kernels can also be chosen as pre-dictionaries. Furthermore, multidimensional kernels representing stochastic processes have also been investigated. For more information, please refer to [33].

To compare various methods more clearly, Table 1 lists different methods to expand stochastic processes, including SPOAFD and POAFD-Chaos methods, as newly proposed in this paper.

The following section provides detailed simulation algorithms for the method proposed in this study.

4. Simulation of non-Gaussian stochastic processes by AFD-type methods

Among others, Zheng gave a method [26] that successfully produces any required number of sample paths at any set of discrete time points that provide a discrete solution to the two-match problem. He later combined his sampling method with the KL and PC expansions to give continuous form stochastic process solutions to solve the two-match problem. The present paper aims to propose AFD-type methods to solve the problem. We only adopt the Zheng's sampling method, while using SPOAFD and POAFD-Chaos to replace the KL and PC methods in Zheng's paper. For the self-containing purpose, we will briefly recall Zheng's algorithm in the following subsection.

4.1. Simulation of discrete-time stochastic samples of Zheng

Assume that a stochastic process $f(t,\omega)$ is specified by its marginal distribution function $G(y;t)$ and its covariance function $\mathbf{C}(s,t)$. Recall that the goal of two-match problems is re-constructing $f(t,\omega)$ from $G(y;t)$ and $\mathbf{C}(s,t)$. Zheng [26] proposes a method by which a set of sample paths satisfying the target marginal distribution function are first found. Afterward, through an iterative procedure, while keeping the marginal distribution unchanged, a sequence of sample paths of the identical marginal distributions converges to one that satisfies the covariance condition. In such a way, the accuracy and efficiency of the simulation only depend on matching the target covariance function. The algorithm corresponding to Zheng's method is summarized in Algorithm 1.

Algorithm 1 Simulation method of stochastic samples.

1: Discretize the spatial domain $t=\{t_1,t_2,\cdots,t_M\}$ and generate samples of random variables as $\mathbf{Y}^{(0)}=\left\{f(t_1,\omega_j),f(t_2,\omega_j),\cdots,f(t_M,\omega_j)\right\}_{j=1}^{N}$ $(f(t_i,\cdot)\sim G(y,t_i),$ $i=1,\cdots,M)$, where N is the sample size.
2: Compute the upper triangular matrix $\mathbf{P}$ by use of a Cholesky decomposition of the target covariance function $\mathbf{C}=\mathbf{P}^T\mathbf{P}$.
3: Compute the simulated covariance matrix $\mathbf{T}^{(0)}$ of samples of random variables $\mathbf{Y}^{(0)}$

$$\mathbf{T}^{(0)}=\frac{\left(\mathbf{Y}^{(0)}\right)^T\mathbf{Y}^{(0)}}{N-1}-\frac{\left(\mathbf{Y}^{(0)}\right)^T\mathbf{U}\mathbf{U}^T\mathbf{Y}^{(0)}}{N(N-1)},\ \text{where } \mathbf{U}=[1]_{N\times 1}. \tag{34}$$

4: Compute the upper triangular matrix $\mathbf{Q}^{(0)}$ by use of a Cholesky decomposition of the target covariance function $\mathbf{T}^{(0)}=\left(\mathbf{Q}^{(0)}\right)^T\mathbf{Q}^{(0)}$.
5: Compute $\tilde{\mathbf{Y}}^{(0)}$ through $\tilde{\mathbf{Y}}^{(0)}=\mathbf{Y}^{(0)}\left(\mathbf{Q}^{(0)}\right)^{-1}\mathbf{P}$.
6: Reorder samples in each column of $\mathbf{Y}^{(0)}$ following the ranking of the realizations in each column of $\tilde{\mathbf{Y}}^{(0)}$. The rearranged matrix is $\mathbf{Y}^{(1)}$.
7: Compute the simulated covariance matrix $\mathbf{T}^{(1)}$ of $\mathbf{Y}^{(1)}$ by (34)
8: Repeat steps 4 through 7 until $\left\|\mathbf{T}^{(k)}-\mathbf{C}\right\|/\|\mathbf{C}\|<\varepsilon$, where k is iteration number.

The key steps are the fifth and sixth steps of Algorithm 1. Sample realizations $\{f(t_i,\omega_j)\}_{j=1}^{N}$ in each column of $\tilde{\mathbf{Y}}$ in the fifth step of Algorithm 1 are different from those in each column of $\mathbf{Y}$ due to the factor matrix $\mathbf{Q}^{-1}\mathbf{P}$. Through the following Proposition 4, we know that the simulated covariance $\tilde{\mathbf{T}}$ of $\tilde{\mathbf{Y}}$ in step 5 is equal to the target covariance function $\mathbf{C}$. However, the elements in each column of $\tilde{\mathbf{Y}}$ change with the updated factor matrix $\mathbf{Q}^{-1}\mathbf{P}$ but do not match the marginal distribution function $F(y,t_i)$. Reordering the sample elements will not change the distributions of random variables but will change the simulated covariance matrix. Hence, by repeating step 6 of Algorithm 1, the simulated covariance functions in the process are getting closer to the target covariance function.

Proposition 4 ([26]). *Consider the upper triangular matrices* $\mathbf{Q}$ *and* $\mathbf{P}$ *obtained by the Cholesky decompositions* $\mathbf{C}=\mathbf{P}^T\mathbf{P}$ *and* $\mathbf{T}=\mathbf{Q}^T\mathbf{Q}$. *The simulated covariance matrix* $\tilde{\mathbf{T}}$ *of the sample matrix* $\tilde{\mathbf{Y}}$, *obtained by* $\tilde{\mathbf{Y}}=\mathbf{Y}\mathbf{Q}^{-1}\mathbf{P}$, *satisfies* $\tilde{\mathbf{T}}=\mathbf{C}$.

Algorithm 1 provides an efficient procedure to simulate samples of stochastic processes. It is desirable to develop methods to represent the stochastic process further. In article [26], Zheng combines Algorithm 1 with KL expansion, PC expansion, and KL+PC expansion to construct continuous stochastic processes solving the two-match problem. The primary study of this article, as shown

Table 2
Relative errors of sample paths and covariance matrix of different terms.

Simulated method	KL				SPOAFD			
term	1	9	19	29	1	9	19	29
1st sample path	0.9828	0.0097	2×10^{-4}	7×10^{-5}	0.2877	0.0009	2×10^{-4}	8×10^{-5}
31st sample path	0.6744	0.0103	2×10^{-4}	5×10^{-5}	0.4619	0.0006	1×10^{-4}	8×10^{-5}
1st row of covariance matrix	0.9331	0.0009	7×10^{-4}	7×10^{-4}	0.737	0.0024	8×10^{-4}	7×10^{-4}
31st row of covariance matrix	0.362	8×10^{-5}	6×10^{-5}	6×10^{-5}	0.601	2×10^{-5}	2×10^{-5}	5×10^{-5}

below, is to show that based on Algorithm 1 AFD-type algorithms and their corresponding chaos forms, as well as their combined use, can replace the KL and PC methods with the same effectiveness and efficiency to solve the two-match problem.

4.2. The SPOAFD method based on stochastic samples

The SPOAFD method is used to recover the corresponding continuous-type stochastic signals. Note that the expansion is with respect to an adaptive system in the $\mathcal{T}$ space. We use the maximal selection principle to get the optimal parameters (20). The algorithm steps are given by Algorithm 2.

Algorithm 2 Algorithm based on stochastic samples and SPOAFD method.

1: Generate stochastic samples $\left\{\left\{f(t_i,\omega_j)\right\}_{j=1}^{N}\right\}_{i=1}^{M}$ of the stochastic process $f_\omega(t)$ using Algorithm 1.

2: The simulated covariance function of stochastic samples $\left\{\left\{f(t_i,\omega_j)\right\}_{j=1}^{N}\right\}_{i=1}^{M}$ can be given as follows

$$\hat{\mathbf{C}}(s,t)=\frac{1}{N-1}\sum_{j=1}^{N}\left[f(t,\omega_j)-\mu(t)\right]\left[f(s,\omega_j)-\mu(s)\right],$$

where $s,t\in\{t_1,\cdots,t_M\}$.

3: Introduce the Poisson kernel K_q, $q\in\mathbf{D}$. The parameters $\{q_k\}_{k=1}^{n}$ are selected by the SPOMSP (20)

$$q_k=\arg\max_{q\in\mathbf{D}}\hat{\mathbb{E}}_\omega\left|\langle f_0(\cdot,\omega_j),E_k^q\rangle\right|^2, \tag{35}$$

where

$$\hat{\mathbb{E}}_\omega\left|\langle f_0(\cdot,\omega_j),E_k^q\rangle\right|^2:=\int_{\partial\mathbf{D}}\int_{\partial\mathbf{D}}\hat{\mathbf{C}}(s,t)\overline{E_k^q}(t)E_k^q(s)dtds, \tag{36}$$

and the $\{E_k^q\}$ is the k-th term of the G-S orthonormal system generated by the kernels $K_{q_1},\cdots,K_{q_{k-1}},K_q$. Computation of the G-S orthonormalization of E_k (or $E_k^{q_k}$) is according to

$$E_k=\frac{K_{q_k}-\sum_{j=1}^{k-1}\langle K_{q_k},E_j\rangle E_j}{\sqrt{\|K_{q_k}\|^2-\sum_{j=1}^{k-1}\left|\langle K_{q_k},E_j\rangle\right|^2}}.$$

4: The non-Gaussian stochastic process can simulate in the following form

$$\hat{f}_0(t,\omega)=\sum_{k=1}^{n}\langle f_0(t,\omega),E_k\rangle E_k(t).$$

In step 3 of Algorithm 2, the parameters are adaptively selected by SPOMSP, where the optimization problem (35) can be approximately solved by exhaustive testing based on a finite pre-sampled subset of $\mathbf{D}$ as the candidate of q. To compute the integral in (36), notice that we only have access to $\hat{\mathbf{C}}(s,t)$ for $s,t\in\{t_i\}_{i=1}^{M}$, we shall perform numerical integration, e.g., trapezoid rule, based on these grid points.

Remark 2 (*Computational Complexity of Algorithm 2 for SPOAFD*)**.** The computational complexity of step 2 is $O(M^2N)$, where M is number of time steps and N is sample size. 'As for step 3 in Algorithm 2, let $N_{\mathbf{D}}$ denote the number of candidates of $q\in\mathbf{D}$ considered in the SPOMSP, finding each q_k in (36) takes a total of $O(M^2N_{\mathbf{D}})$ operations in exhaustive testing and $O(nMN_{\mathbf{D}})$ operations in performing the G-S orthonormalization. Since, in practice, we have $n\ll N,\ M$, the overall computational complexity of Algorithm 2 is $O(M^2N+nM^2N_{\mathbf{D}})$, consisting of evaluating the simulated covariance matrix via Monte Carlo and SPOMSP. In KL expansion, we need to compute the simulated covariance matrix $[\hat{\mathbf{C}}(t_i,t_j)]_{i,j=1,\ldots,M}$ (same as in step 2 of Algorithm 2) and solve the eigenvalue problem (up to order-n). A general estimation gives that the computational complexity is $O(M^2N+nM^3)$. Therefore, when $N_{\mathbf{D}}$ (number of Poisson kernels considered in the SPOMSP) and M (number of time steps) share a similar scale, the SPOAFD method shown in Algorithm 2 has a similar computational complexity as KL expansion.

Algorithm 2 provides an efficient method to expand stochastic samples obtained from Algorithm 1. The optimal parameters can be selected based on the sampling points $f(t_i,\omega_j)$ obtained from Algorithm 1 of the stochastic process. Those parameters are used to generate a corresponding continuous type solution of the two-match problem. Through comparison, Section 5 shows that the simulation is accurate with efficient. The main computational error of this algorithm is caused by G-S orthonormalization.

4.3. The POAFD-Chaos method based on stochastic samples

This method uses the adaptive random Poisson kernel to represent the stochastic process. The idea of this method is similar to the PC method. Note that this time we expand with respect to a chaos system where the coefficients are functions of the variable t. The algorithm is given in Algorithm 3.

Algorithm 3 Algorithm based on stochastic samples and adaptive POAFD-Chaos method.

1: Generate stochastic samples $\left\{\left\{f(t_i,\omega_j)\right\}_{j=1}^{N}\right\}_{i=1}^{M}$ of the stochastic process $f_\omega(t)$ using Algorithm 1.

2: Generate N samples following uniform distribution on $[0,2\pi]$, denoted by $\{U(\omega_j)\}_{j=1}^{N}$ and introduce the corresponding stochastic Poisson kernels using (28), i.e. $\left\{P_z\left(U(\omega_j)\right)\right\}_{j=1}^{N}$, where

$$P_z(U(\omega_j))=\frac{1-|z|^2}{\left|z-e^{iU(\omega_j)}\right|^2},$$

parameterized by $z\in\mathbf{D}$

3: The parameters $\{z_k\}_{k=1}^{n}$ are selected by the SPOMSP (27),

$$z_k=\arg\sup_z\left\{\sup_{i=1,\cdots,M}\mathbb{E}_\omega\left[\left|f_0(t_i,\omega)E_k^z(U(\omega))\right|^2\right]\;\middle|\;z\in\mathbf{D}\right\},\tag{37}$$

where the $\{E_k^z\}$ is the k-th term of the G-S orthonormal system generated by the kernels $P_{z_1},\cdots,P_{z_{k-1}},P_z$. Computation of the G-S orthonormalization of E_k (or $E_k^{z_k}$) is according to

$$E_k=\frac{P_{z_k}-\sum_{j=1}^{k-1}\langle P_{z_k},E_j\rangle E_j}{\sqrt{\|P_{z_k}\|^2-\sum_{j=1}^{k-1}\left|\langle P_{z_k},E_j\rangle\right|^2}}.$$

4: Compute the coefficient $g_k(t_i)=\mathbb{E}_\omega\left[f_0(t_i,\omega_j)E_k\left(U(\omega_j)\right)\right]$ by the expansion (33).

5: The non-Gaussian stochastic process is expanded

$$f_0(t_i,\omega)=\sum_{k=1}^{n}g_k(t_i)E_k\left(U(\omega)\right),\ i=1,\cdots,M.\tag{38}$$

The SPOMSP (37) in Algorithm 3 involves a two-layer optimization problem whose target function is defined as the supremum of the expectation over $\{t_i\}_{i=1}^{M}$. Same as in Algorithm 2, we estimate the expectation in (37) using Monte Carlo and solve (37) via exhaustive testing over candidate points in $\mathbf{D}$. In particular, following the relation in (14), we have

$$\mathbb{E}_\omega\left[\left|f_0(t_i,\omega)E_k^z(U(\omega))\right|^2\right]=\mathbb{E}_X\left[\left|F_{f_0(t_i)}^{-1}(F_U(U))E_k^z(U)\right|^2\right]\approx\frac{1}{N}\sum_{j=1}^{N}\left|\hat{F}_{f_0(t_i)}^{-1}\left(\frac{U(\omega_j)}{2\pi}\right)E_k^z(U(\omega))\right|^2,$$

where $\hat{F}_{f_0(t)}$ denotes the empirical estimate of the CDF function $F_{f_0(t)}$ based on the samples in step 1.

Remark 3 (*Computational Complexity of Algorithm 3 for POAFD-Chaos*)**.** Performing a similar computational complexity analysis as for Algorithm 2, we obtain $O(nMNN_{\mathbf{D}})$ as the computational complexity of Algorithm 3, which is mainly contributed by the exhaustive parameter testing in SPOMSP (37). Compared with the computational complexity of order-n PC, $O(nMN)$, the POAFD-Chaos method is more expensive. In PC methods, the basis functions are pre-selected based on the orthogonal polynomials, while the POAFD-Chaos method adaptively chooses the basis functions driven by the SPOMSP. As benefit we gain efficiency, explicitness and accuracy of the approximation. In PC methods, the basis functions are pre-selected based on the orthogonal polynomials, while the POAFD-Chaos method adaptively chooses the basis functions driven by the SPOMSP. In other words, we trade computational efficiency for flexibility and effectiveness of the expansion formula.

The following section will demonstrate the performance of the proposed algorithm through numerical experiments in which Algorithm 2 is mainly compared with the KL method, and Algorithm 3 is primarily compared with the PC method.

5. Numerical examples

We will work with four numerical examples of stationary and non-stationary and strongly and weakly non-Gaussian processes to verify the effectiveness of SPOAFD and POAFD-Chaos for expanding non-Gaussian stochastic processes. Each example uses Algorithm 2 SPOAFD and Algorithm 3 POAFD-Chaos to simulate the corresponding non-Gaussian processes. Among them, Algorithm 2 means to be compared with KL, and Algorithm 3 is compared with Hermite PC. The first step for all models is to use Algorithm 1 with

five iterations to generate random samples. In addition, the number of non-Gaussian sample points of each random variable for a fixed time t_i by Zheng's method is 10 000. To resolve the Gibbs phenomenon, we adopt the methods of first compressing the graph from $(0, 2\pi)$ to $(0, \pi)$ and then extending back to $(0, 2\pi)$ symmetrically with respect to the vertical line at $t = \pi$. To apply Algorithm 2 SPOAFD, for the first two weakly non-Gaussian examples and the last two strongly non-Gaussian examples, the time interval $[0, 2\pi]$ is equally discretized into 64 and 32 parts, respectively. To use Algorithm 3 POAFD-Chaos, for the first two weak non-Gaussian examples, the interval $[0, 2\pi]$ is discretized into equally 40 parts, and the third non-Gaussian example into 30 parts, and the last non-Gaussian example into 20 parts.

Example 5.1 (*Stationary Weakly Non-Gaussian Process*)**.** The marginal non-Gaussian cumulative distribution function (CDF) is assumed to be the Beta distribution, with the formula

$$G(y; p, q) = \frac{\Gamma(p+q)}{\Gamma(p)\Gamma(q)} \int_0^u z^{p-1}(1-z)^{q-1} dz \tag{39}$$

where $\Gamma(\cdot)$ is the Gamma function, and

$$u = \frac{y - y_{min}}{y_{max} - y_{min}} \tag{40}$$

with the upper and lower bounds y_{max} and y_{min}. The distribution parameters are $p = 4$ and $q = 2$ so that the mean is zero and the variance is one. The upper and lower bounds of the distribution are, respectively, $y_{min} = -3.74$ and $y_{max} = 1.87$. The target Beta distribution is weakly non-Gaussian. The correlation distortion of this beta distribution is small [46]. The target covariance function is

$$\mathbf{C}(s,t) = e^{-(s-t)^2}, \quad \forall s, t \in [0, 2\pi]. \tag{41}$$

Without loss of general, the 1st and 31st sample paths and the 1st and 31st rows of the covariance matrix are selected in Fig. 2 to compare the approximation of the partial sum of the truncated KL (8) and the truncated SPOAFD (25) expansions at $n = 9$ and $n = 29$, respectively. In (a), the top graph illustrates the simulation of the sample path using 9 partial sums of KL (blue line) and SPOAFD (red line), while the bottom graph shows the simulation using 29 partial sums of KL and SPOAFD. (b) also depicts different sample paths using KL and SPOAFD simulations. On the other hand, (c) and (d) represent the simulation of covariance, with the dashed line representing the target covariance function. The green line shows the sampling points found by Algorithm 1, the blue line represents the covariance simulated using the KL method, and the red line represents the covariance simulated using the SPOAFD method. The relative errors of the 1st and 31st sample paths and the 1st and 31st row of the covariance matrix are given in Table 2, respectively. At the 29th partial sums, both SPOAFD and KL expansions approximately recover the stochastic process with Zheng's realizations and the target covariance function. In local details, it can be observed that the SPOAFD method seems to be better than the KL method. It can be seen that Algorithm 2 SPOAFD has good convergence, resulting in high precision to simulate stationary non-Gaussian stochastic processes. When higher-order partial sums are involved, SPOAFD performs better than KL in the example. The Table 2 exhibits two more partial sum results.

Next, we test the POAFD-Chaos method with the same stochastic process as in Example 5.1. We compare two methods. One is the POAFD-Chaos expansion, where the partial sum order $n = 40$, as used in the formula (32), and the other is PC, where the order of the one-dimensional Hermite polynomials is adopted as 5. The comparison between the target, the PC-simulated covariance, and the POAFD-Chaos-simulated covariance are shown in Fig. 3, which demonstrates the high accuracy of the proposed Algorithm 3.

The marginal distribution function of a stationary stochastic process does not change with time. However, the marginal distribution of a non-stationary process varies with the time change. In Example 5.2, we observe the high accuracy of the new algorithm in simulating non-Gaussian stochastic processes under non-stationary conditions.

Example 5.2 (*Non-stationary Weakly Non-Gaussian Process*)**.** The example is also chosen as the Bata marginal distribution function in (39). The target marginal distribution function changes with t. We can be rewrite (40) in this form

$$u(t) = \frac{y(t) - y_{min}(t)}{y_{max}(t) - y_{min}(t)} \tag{42}$$

where

$$y_{min}(t) = \mu_B(t) - \sigma_B(t)\sqrt{\frac{p(p+q+1)}{q}}, \tag{43}$$

$$y_{max}(t) = \mu_B(t) + \sigma_B(t)\sqrt{\frac{q(p+q+1)}{p}}. \tag{44}$$

The covariance is based on the non-stationary Brown-Bridge covariance model. In the non-stationary case, the variance is related to t. The Brown-Bridge covariance function is given by

$$\mathbf{C}(s,t) = min(s,t) - \frac{st}{2\pi}, \quad \forall s, t \in [0, 2\pi] \tag{45}$$

and the variance is obtained to be

$$\sigma_B^2(t) = \mathbf{C}(t,t) = min(t,t) - \frac{st}{2\pi} = t - \frac{t^2}{2\pi}, \quad \forall t \in [0, 2\pi] \tag{46}$$

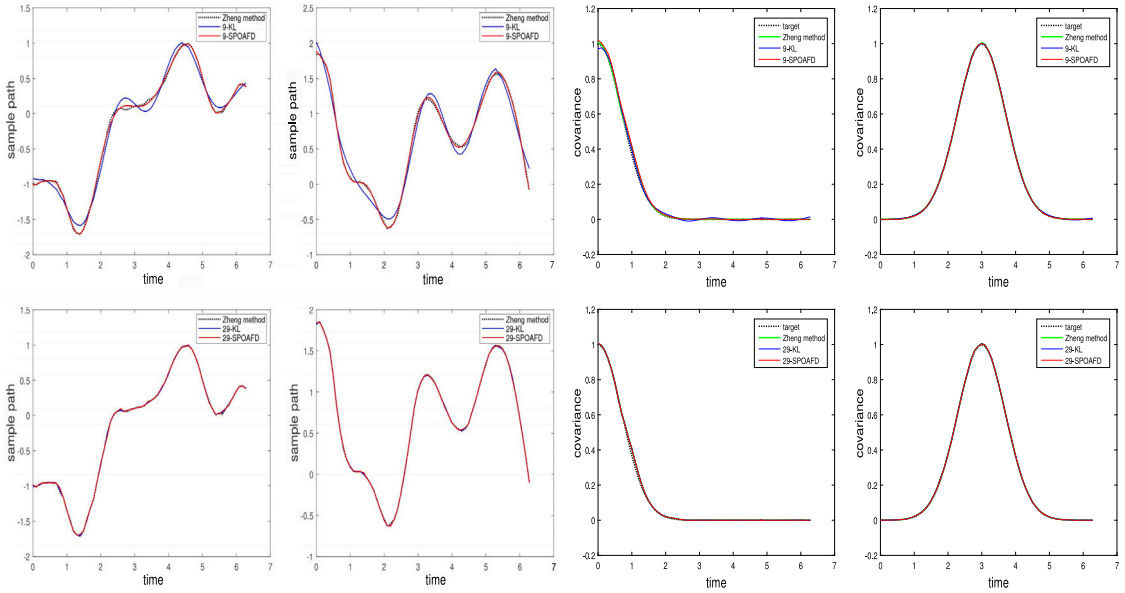

(a) 1st sample path (b) 31st sample path (c) 1st row of covariance matrix (d) 31st row of covariance matrix

Fig. 2. Simulation of 9 and 29 partial sums by KL and SPOAFD.

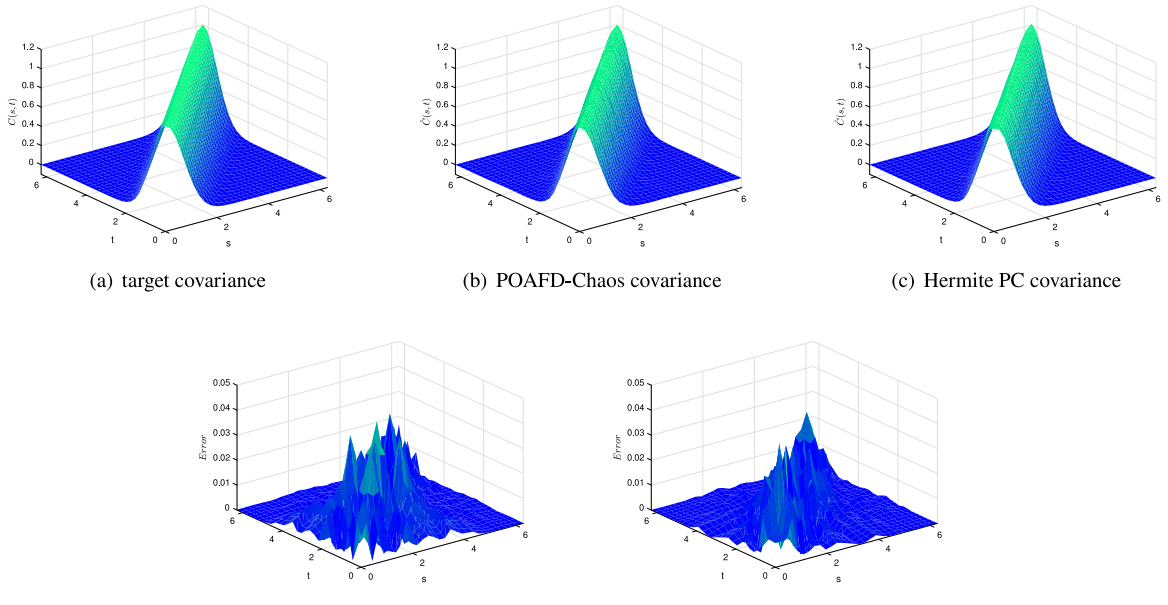

(a) target covariance (b) POAFD-Chaos covariance (c) Hermite PC covariance

(d) relative error between target and POAFD-Chaos covariance (e) relative error between target and Hermite PC covariance

Fig. 3. Comparison between target covariance (a), POAFD-Chaos-simulated covariance (b), and Hermite PC-simulated covariance (c); and the relative errors between target and POAFD-Chaos-simulated covariance (d), target and Hermite PC-simulated covariance (e).

In this example, we also choose $p = 4$, $q = 2$. We set $\mu_B(t)$ to be zero for convenience. Solving (43) and (44) yields,

$$y_{min}(t) = -\sqrt{14(t - \frac{t^2}{2\pi})},\ y_{max}(t) = \sqrt{3.5(t - \frac{t^2}{2\pi})}. \tag{47}$$

Without loss of the generality, the 2000th and 4000th sample paths and the 20th and 40th rows of the covariance matrix are selected in Fig. 4 to compare the approximation of the partial sum of the truncated KL (8) and the truncated SPOAFD (25) expansions at $n = 24$ and $n = 64$, respectively. The relative errors of the 2000th and 4000th sample paths and the 20th and 40th rows of the

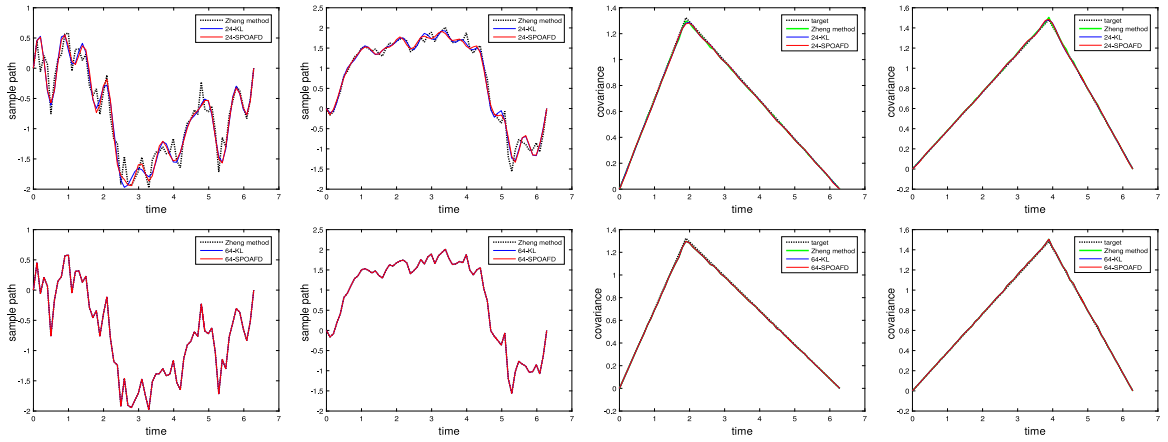

(a) 2000th sample path (b) 4000th sample path (c) 20th row of covariance matrix (d) 40th row of covariance matrix

Fig. 4. Simulation of 24 and 64 partial sums by KL and SPOAFD.

Table 3
Relative errors of sample paths and covariance matrix of different terms.

Simulated method	KL				SPOAFD			
term	4	24	44	64	4	24	44	64
2000th sample path	0.1306	0.0185	0.0072	2×10^{-31}	0.1148	0.0199	0.0021	6×10^{-10}
4000th sample path	0.0452	0.0075	0.0012	3×10^{-31}	0.1499	0.0091	0.0007	2×10^{-10}
20th row of covariance matrix	0.0035	0.0002	0.0001	2×10^{-4}	0.0684	0.0001	0.0001	2×10^{-4}
40th row of covariance matrix	0.0016	8×10^{-5}	8×10^{-5}	9×10^{-5}	0.0460	9×10^{-5}	8×10^{-5}	9×10^{-5}

covariance matrix are given in Table 3, respectively. Comparison between target, PC-simulated covariance, and POAFD-Chaos-simulated covariance are shown in Fig. 5. The number of the partial sum selected for the POAFD-Chaos method is 40. Moreover, we adopt the 5-order Herimite PC system. The experiment shows that AFD-type methods can simulate non-Gaussian stochastic processes under non-stationary conditions and achieve excellent results.

Example 5.3 (*Stationary Strongly Non-Gaussian Process*)**.** The marginal non-Gaussian cumulative distribution function in the third example is shifted log-normal distribution, with the CDF given by

$$G(y;\mu,\sigma,\delta) = \Phi\left(\frac{ln(y-\delta)-\mu}{\sigma}\right) \tag{48}$$

The distribution parameters $\mu = -0.7707$, $\sigma = 1$, and $\delta = -0.7628$ are selected to produce zero mean and unit variance. The target shifted log-normal distribution is considered strongly non-Gaussian and deviates significantly from the Gaussian case [46,47].

And the target covariance function is given by the absolute value exponential covariance function,

$$\mathbf{C}(s,t) = e^{-|s-t|}, \quad \forall s,t \in [0,2\pi]. \tag{49}$$

To evaluate the accuracy of the KL and SPOAFD expansions, we selected the 1st and 5000th sample paths and the 1st and 10th rows of the covariance matrix for comparison purposes. The results of our analysis are presented in Fig. 6. Specifically, we compared the performance of the truncated KL expansion (8) and the truncated SPOAFD expansion (25) at $n = 16$ and $n = 32$, respectively. Remarkably, at the 32nd partial sum, both the SPOAFD and KL expansions could recover the target covariance function with high precision. To quantify the accuracy of our methods, we computed the relative errors of the 1st and 5000th sample paths and the 1st and 10th rows of the covariance matrix. The results of our analysis are presented in Table 4, which clearly illustrates the trend of decreasing relative error with the increasing number of terms.

To further investigate the performance of our methods, we compared the target covariance (a), POAFD-Chaos-simulated covariance (b), and Hermite PC-simulated covariance (c) in Fig. 7. For this purpose, we selected a partial sum of 30 for the POAFD-Chaos method and adopted a 3-order Herimite PC system. We compared the relative errors between the POAFD-Chaos-simulated and target covariance (d) and between the Hermite PC-simulated and target covariance (e). The results indicate that our method achieves a comparable level of accuracy to Hermite PC. Furthermore, our approach provides an adaptive sparse representation, which offers more flexibility and convenience than the system selection process required by PC.

Example 5.4 (*Non-stationary Strongly Non-Gaussian Process*)**.** The marginal distribution function is also the shifted lognormal in (48). In the non-stationary non-Gaussian case, the target marginal distribution function varies with t. In this case, the shape of the

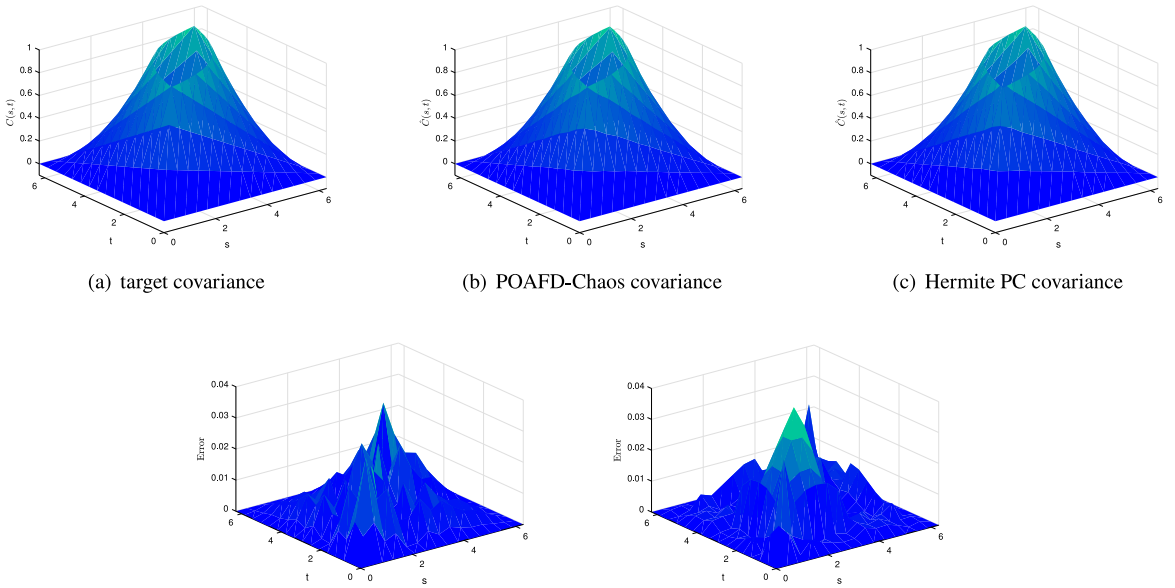

(a) target covariance (b) POAFD-Chaos covariance (c) Hermite PC covariance

(d) relative error between target and POAFD-Chaos covariance (e) relative error between target and Hermite PC covariance

Fig. 5. Comparison between target covariance (a), POAFD-Chaos-simulated covariance (b), and Hermite PC-simulated covariance (c); and the relative errors between target and POAFD-Chaos-simulated covariance (d), target and Hermite PC-simulated covariance (e).

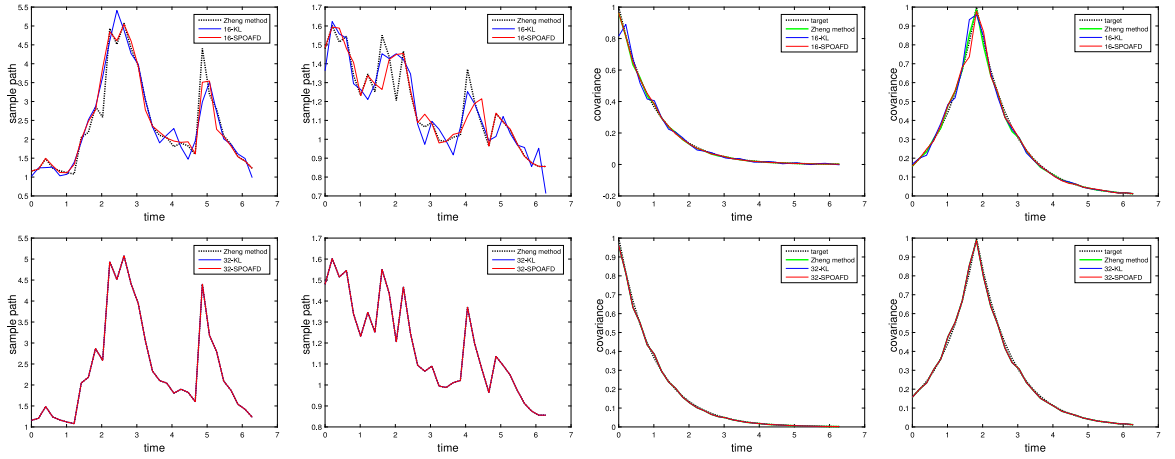

(a) 1st sample path (b) 5000th sample path (c) 1st row of covariance matrix (d) 10th row of covariance matrix

Fig. 6. Simulation of 16 and 32 partial sums by KL and SPOAFD.

Table 4
Relative errors of sample paths and covariance matrix of different terms.

Simulated method	KL				SPOAFD			
term	8	16	24	32	8	16	24	32
1st sample path	0.0249	0.0118	0.0056	2×10^{-31}	0.0266	0.0050	0.0019	4×10^{-20}
5000th sample path	0.0041	0.0019	9×10^{-4}	2×10^{-31}	0.0050	0.0012	3×10^{-4}	3×10^{-20}
1st row of covariance matrix	0.0309	0.0098	0.0041	7×10^{-4}	0.0003	0.0005	0.0007	7×10^{-4}
10th row of covariance matrix	0.0117	0.0023	0.0015	0.0010	0.0184	0.0016	0.0012	0.0010

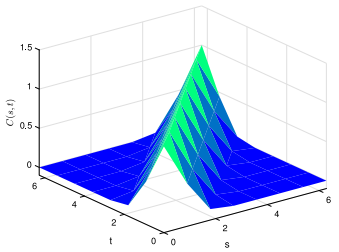

(a) target covariance

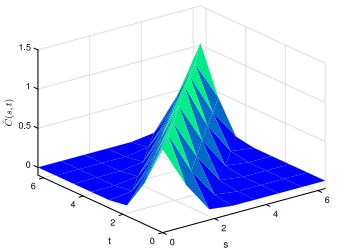

(b) POAFD-Chaos covariance

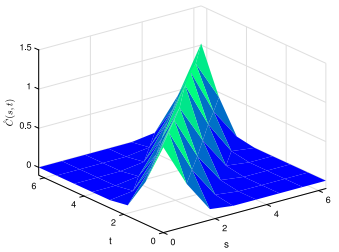

(c) Hermite PC covariance

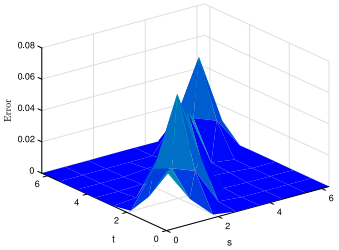

(d) relative error between target and POAFD-Chaos covariance

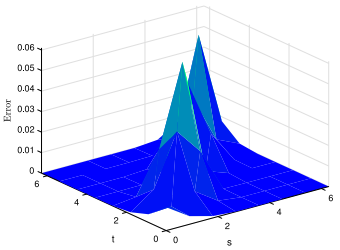

(e) relative error between target and Hermite PC covariance

Fig. 7. Comparison between target covariance (a), POAFD-Chaos-simulated covariance (b), and Hermite PC-simulated covariance (c); and the relative errors between target and POAFD-Chaos-simulated covariance (d), target and Hermite PC-simulated covariance (e).

Table 5
Relative errors of sample paths and covariance matrix of different terms.

Simulated method	KL				SPOAFD			
term	8	16	24	32	8	16	24	32
10 000th sample path	0.0065	4×10^{-4}	1×10^{-6}	1×10^{-31}	0.0007	8×10^{-5}	4×10^{-7}	2×10^{-19}
55 050th sample path	0.0250	2×10^{-4}	8×10^{-6}	1×10^{-31}	0.0166	3×10^{-5}	8×10^{-7}	2×10^{-16}
1st row of covariance matrix	0.0101	0.0101	0.0101	0.0101	0.0100	0.0100	0.0101	0.0101
9th row of the covariance matrix	0.0042	0.0024	0.0024	0.0024	0.0160	0.0024	0.0024	0.0024

distribution is given by σ, which is usually set to 1. Similarly, The parameters μ and σ can be represented by the mean and variance of this distribution (48).

$$\mu_{SL}(t) = \delta(t) + e^{\mu(t)+\frac{\sigma^2}{2}} \tag{50}$$

$$\sigma_{SL}(t) = (e^{\sigma^2} - 1)e^{2\mu(t)+\sigma^2} \tag{51}$$

The target covariance function is the exponential covariance function,

$$\mathbf{C}(s,t) = e^{-(s+t)-|s-t|}, \quad \forall s,t \in [0, 2\pi]$$

The variance function is

$$\sigma_{SL}^2(t) = \mathbf{C}(t,t) = e^{-(t+t)-|t-t|} = e^{-2t}, \quad \forall t \in [0, 2\pi].$$

For simplicity, let $\mu_{SL} = 0$ and $\sigma = 1$. Solving (50) and (51) yield

$$\mu(t) = -t - ln\sqrt{e(e-1)},\ \sigma(t) = (e^{\sigma^2} - 1)e^{2\mu(t)+\sigma^2}. \tag{52}$$

Without loss of the generality, the 10 000th and 5050th sample paths and the 1st and 9th rows of the covariance matrix are selected in Fig. 8 to compare the approximation of the partial sum of the truncated KL (8) and the truncated SPOAFD (25) expansions at $n = 8$ and $n = 32$, respectively. At the 32nd partial sums, both SPOAFD and KL expansions fully coincide with Zheng's discrete sample paths. The Table 5 gives relative errors of the 1000th and 5050th sample paths and the 1st and 9th rows of the covariance matrix. Comparison between target, PC-simulated covariance, and POAFD-Chaos-simulated covariance are shown in Fig. 9. The partial sum order for the POAFD-Chaos method is 20. We adopt the 6-order Herimite PC system.

Our method has shown to be highly effective in simulating strongly non-stationary non-Gaussian processes, further emphasizing its versatility and adaptability. Based on the four examples presented above, it is evident that both SPOAFD and POAFD-Chaos methods are highly applicable to non-Gaussian processes, offering efficient and accurate simulation capabilities.

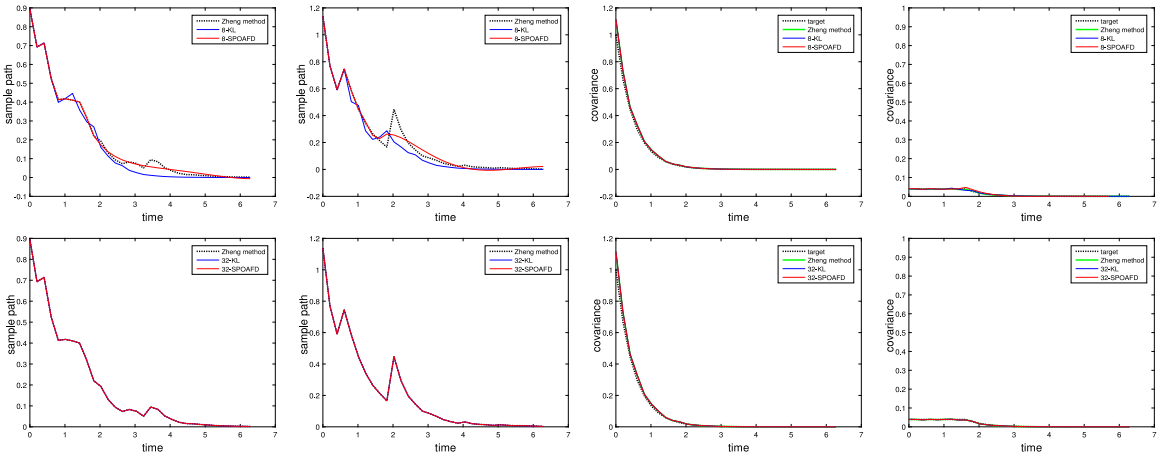

(a) 10000th sample path (b) 5050th sample path (c) 1st row of covariance matrix (d) 9th row of covariance matrix

Fig. 8. Simulation of 8 and 32 partial sums by KL and SPOAFD.

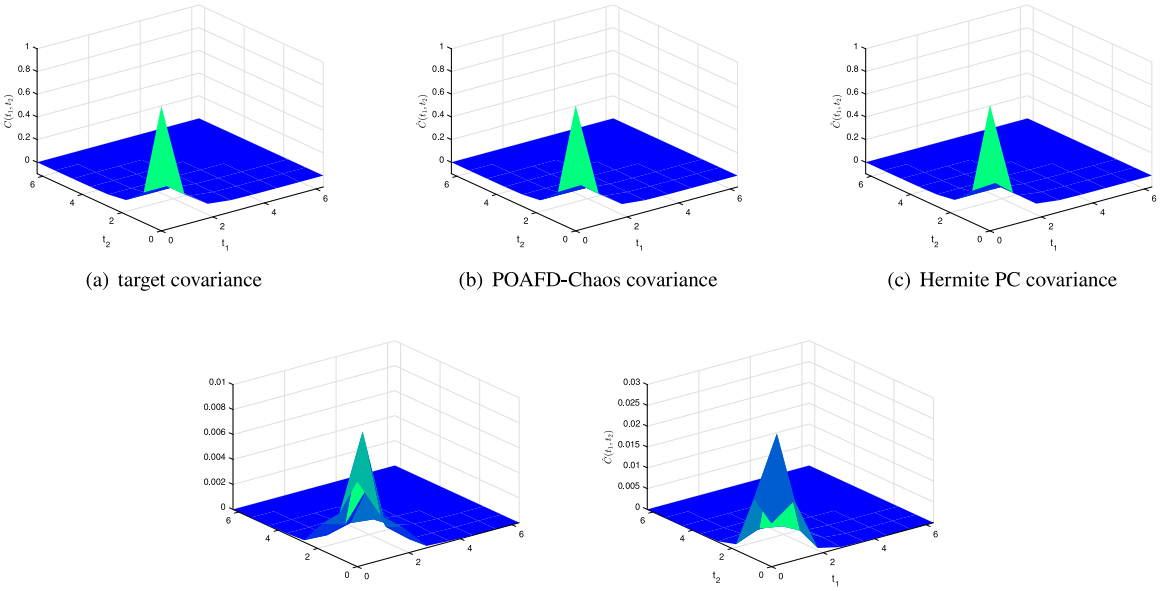

(a) target covariance (b) POAFD-Chaos covariance (c) Hermite PC covariance

(d) relative error between target and POAFD-Chaos covariance (e) relative error between target and Hermite PC covariance

Fig. 9. Comparison between target covariance (a), POAFD-Chaos-simulated covariance (b), and Hermite PC-simulated covariance (c); and the relative errors between target and POAFD-Chaos-simulated covariance (d), target and Hermite PC-simulated covariance (e).

6. Conclusion

This paper presents two new methods, SPOAFD and POAFD-Chaos, for simulating non-Gaussian stochastic processes specified by covariance and marginal distribution functions. Such a two-match problem is usually solved first by obtaining a group of random samples at discrete times and then using KL, PC, or their combinations to get continuous time approximations of the whole stochastic process. This paper introduces the AFD-type methods to replace KL and PC and thus offers a uniform treatment in the second step with at least equal power and efficiency. Not only in solving the two-match problem, the methodology itself has certain advantages. The new algorithms do not need to compute the eigenvalues and the eigenfunctions of the integral operator defined by the covariance kernel that, compared with the KL method, significantly reduces computation complexity and saves computer consumption. Compared with the PC method, our AFD-Chaos also possesses the adaptive feature. The advantage is that it offers a great deal of flexibility and efficiency. At the same time, the AFD-type methods have analytical representations for non-Gaussian stochastic processes. The AFD-type algorithms can also be extended to multi-variate random fields.

Declaration of competing interest

The authors declare the following financial interests/personal relationships which may be considered as potential competing interests: Tao Qian reports was provided by Macau University of Science and Technology. Tao Qian reports a relationship with Macau University of Science and Technology that includes: employment.

Data availability

No data was used for the research described in the article.

Acknowledgments

This work was supported by Zhejiang Provincial Natural Science Foundation of China [grant number LQ23A010014], Research grant of Macau University of Science and Technology [grant number FRG-22-075-MCMS], and Macao Government Research Funding [grant number FDCT0128/2022/A].

References

[1] O. Vasicek, An equilibrium characterization of the term structure, J. Financ. Econ. 5 (1977) 177–188, http://dx.doi.org/10.1016/0304-405X(77)90016-2.
[2] S.E. Shreve, Stochastic Calculus for Finance II: Continuous-Time Models, Springer, New York, 2004.
[3] C.L. Stokes, D.A. Lauffenburger, S.K. Williams, Migration of individual microvessel endothelial cells: stochastic model and parameter measurement, J. Cell Sci. 99 (1991) 419–430, http://dx.doi.org/10.1242/jcs.99.2.419.
[4] R.Y. Rubinstein, D.P. Kroese, Simulation and the Monte Carlo Method, John Wiley & Sons, 2016.
[5] M. Shinozuka, G. Deodatis, Simulation of stochastic processes by spectral representation, Appl. Mech. Rev. 44 (1991) 191–204, http://dx.doi.org/10.1115/1.3119501.
[6] S. Huang, S. Quek, K. Phoon, Convergence study of the truncated Karhunen–Loeve expansion for simulation of stochastic processes, Internat. J. Numer. Methods Engrg. 52 (2001) 1029–1043, http://dx.doi.org/10.1002/nme.255.
[7] M.B. Priestley, Non-linear and non-stationary time series analysis, J. R. Stat. Soc. Ser. C Appl. Stat. 39 (1990) 266–268, http://dx.doi.org/10.2307/2347773.
[8] V.A. Mabert, Cases in Manufacturing and Service Systems Management, Prentice Hall, 1991.
[9] P.A. Friberg, C.A. Susch, A User's Guide to STRONGMO: Version 1.0 of NCEER's Strong-Motion Data Access Tool for PCs and Terminals, National Center for Earthquake Engineering Research, 1990.
[10] M.K. Ochi, S.B. Malakar, W.C. Wang, Statistical Analysis of Coastal Waves Observed During the ARSLOE Project, Coastal and Oceanographic Engineering Department, University of Florida, 1982.
[11] T. Stathopoulos, PDF of wind pressures on low-rise buildings, J. Struct. Div. 106 (1980) 973–990, http://dx.doi.org/10.1061/JSDEAG.0005443.
[12] F.C. Moon, Chaotic Vibrations: An Introduction for Applied Scientists and Engineers, Research supported by NSF, 1987.
[13] J.R. Wallis, D.P. Lettenmaier, E.F. Wood, A daily hydroclimatological data set for the continental United States, Water Resour. Res. 27 (1991) 1657–1663, http://dx.doi.org/10.1029/91WR00977.
[14] K.R. Gurley, Modelling and Simulation of Non-Gaussian Processes, University of Notre Dame, 1997.
[15] K.R. Gurley, A. Kareem, A conditional simulation of non-normal velocity/pressure fields, J. Wind Eng. Ind. Aerodyn. 77 (1998) 39–51, http://dx.doi.org/10.1016/S0167-6105(98)00130-5.
[16] M. Grigoriu, On the spectral representation method in simulation, Probab. Eng. Mech. 8 (1993) 75–90, http://dx.doi.org/10.1016/0266-8920(93)90002-D.
[17] M. Grigoriu, Simulation of stationary non-Gaussian translation processes, J. Eng. Mech. 124 (1998) 121–126, http://dx.doi.org/10.1061/(ASCE)0733-9399(1998)124:2(121).
[18] G. Deodatis, R.C. Micaletti, Simulation of highly skewed non-Gaussian stochastic processes, J. Eng. Mech. 127 (2001) 1284–1295, http://dx.doi.org/10.1061/(ASCE)0733-9399(2001)127:12(1284).
[19] P. Bocchini, G. Deodatis, Critical review and latest developments of a class of simulation algorithms for strongly non-Gaussian random fields, Probab. Eng. Mech. 23 (2008) 393–407, http://dx.doi.org/10.1016/j.probengmech.2007.09.001.
[20] M.D. Shields, G. Deodatis, P. Bocchini, A simple and efficient methodology to approximate a general non-Gaussian stationary stochastic process by a translation process, Probab. Eng. Mech. 26 (2011) 511–519, http://dx.doi.org/10.1016/j.probengmech.2011.04.003.
[21] K.K. Phoon, S.P. Huang, S.T. Quek, Simulation of second-order processes using Karhunen–Loeve expansion, Comput. Struct. 80 (2002) 1049–1060, http://dx.doi.org/10.1016/S0045-7949(02)00064-0.
[22] K.K. Phoon, H.W. Huang, S.T. Quek, Simulation of strongly non-Gaussian processes using Karhunen–Loeve expansion, Probab. Eng. Mech. 20 (2005) 188–198, http://dx.doi.org/10.1016/j.probengmech.2005.05.007.
[23] R. Ghanem, The nonlinear Gaussian spectrum of log-normal stochastic processes and variables, J. Eng. Mech. 66 (1999) 964–973, http://dx.doi.org/10.1115/1.2791806.
[24] B. Puig, F. Poirion, C. Soize, Non-Gaussian simulation using Hermite polynomial expansion: convergences and algorithms, Probab. Eng. Mech. 17 (2002) 253–264, http://dx.doi.org/10.1016/S0266-8920(02)00010-3.
[25] S. Sakamoto, R. Ghanem, Polynomial chaos decomposition for the simulation of non-Gaussian nonstationary stochastic processes, J. Eng. Mech. 128 (2002) 190–201, http://dx.doi.org/10.1061/(ASCE)0733-9399(2002)128:2(190).
[26] Z. Zheng, H. Dai, Y. Wang, W. Wang, A sample-based iterative scheme for simulating non-stationary non-Gaussian stochastic processes, Mech. Syst. Signal Process. 151 (2021) 107420, http://dx.doi.org/10.1016/j.ymssp.2020.107420.
[27] T. Qian, Y.B. Wang, Adaptive Fourier series-a variation of greedy algorithm, Adv. Comput. Math. 34 (2011) 279–293, http://dx.doi.org/10.1007/s10444-010-9153-4.
[28] T. Qian, Two-dimensional adaptive Fourier decomposition, Math. Methods Appl. Sci. 39 (2016) 2431–2448, http://dx.doi.org/10.1002/mma.3649.
[29] Q.H. Chen, T. Qian, L.H. Tan, A Theory on Non-Constant Frequency Decompositions and Applications, Advancements in Complex Analysis: From Theory to Practice, Springer International Publishing, 2020, pp. 1–37.
[30] V.N. Temlyakov, Greedy Approximation, Cambridge University Press, 2011.
[31] T. Qian, Sparse representation of random signals, Math. Methods Appl. Sci. 45 (2022) 4210–4230, http://dx.doi.org/10.1002/mma.8033.
[32] T. Qian, Y. Zhang, W. q. Liu, W. Qu, Adaptive Fourier decomposition-type sparse representations versus the Karhunen–Loève expansion for decomposing stochastic processes, Math. Methods Appl. Sci. (2023) http://dx.doi.org/10.1002/mma.9301.
[33] W. Qu, Y. Zhang, T. Qian, A general formulation of chaos and AFD chaos, 2023, preprint.

[34] F. Yang, M. Chen, J. Chen, P.T. Li, W. Qu, J.C. Chen, T. Qian, Sparse series of solutions of random boundary and initial value problems, 2023, http://dx.doi.org/10.48550/arXiv.2112.04132, preprint. arXiv:2112.04132.
[35] T. Qian, Intrinsic mono-component decomposition of functions: An advance of Fourier theory, Math. Methods Appl. Sci. 33 (2010) 880–891, http://dx.doi.org/10.1002/mma.1214.
[36] Y.B. Wang, T. Qian, Pseudohyperbolic distance and n-best rational approximation in H2 space, Math. Methods Appl. Sci. 44 (2021) 8497–8504, http://dx.doi.org/10.1002/mma.7267.
[37] W. Qu, T. Qian, G.T. Deng, A stochastic sparse representation: n-best approximation to random signals and computation, Appl. Comput. Harmon. Anal. 55 (2021) 185–198, http://dx.doi.org/10.1016/j.acha.2021.05.003.
[38] G.J. Lord, C.E. Powell, T. Shardlow, An Introduction to Computational Stochastic PDEs, Cambridge University Press, 2014.
[39] T.Y. Hou, W. Luo, B. Rozovskii, H.M. Zhou, Wiener chaos expansions and numerical solutions of randomly forced equations of fluid mechanics, J. Comput. Phys. 216 (2006) 687–706, http://dx.doi.org/10.1016/j.jcp.2006.01.008.
[40] C. Schwab, R.A. Todor, Sparse finite elements for elliptic problems with stochastic loading, Numer. Math. 95 (2003) 707–734, http://dx.doi.org/10.1007/s00211-003-0455-z.
[41] H.L. Van Trees, Detection, Estimation, and Modulation Theory, Part I: Detection, Estimation, and Linear Modulation Theory, John Wiley & Sons, 2004.
[42] D. Xiu, G.E. Karniadakis, The Wiener-Askey polynomial chaos for stochastic differential equations, SIAM J. Sci. Comput. 24 (2002) 619–644, http://dx.doi.org/10.1137/S1064827501387826.
[43] D. Xiu, Numerical Methods for Stochastic Computations: A Spectral Method Approach, Princeton University Press, 2010.
[44] N. Wiener, The homogeneous chaos, Am. J. Math. 60 (1938) 897–936, http://dx.doi.org/10.2307/2371268.
[45] T. Qian, A novel Fourier theory on non-linear phase and applications, Adv. Math. 47 (2018) 321–347, http://dx.doi.org/10.48550/arXiv.1805.06101.
[46] H. Kim, M.D. Shields, Modeling strongly non-Gaussian non-stationary stochastic processes using the iterative translation approximation method and Karhunen–Loeve expansion, Comput. Struct. 161 (2015) 31–42, http://dx.doi.org/10.1016/j.compstruc.2015.08.010.
[47] K.K. Phoon, S.P. Huang, S.T. Quek, Simulation of second-order processes using Karhunen–Loeve expansion, Comput. Struct. 80 (2002) 1049–1060, http://dx.doi.org/10.1016/S0045-7949(02)00064-0.